

# Modeling and Designing of Active Vibration Isolation Platform

Valery Mikhailov<sup>1\*</sup>, Alexey Kopylov<sup>2</sup>, Alexander Kazakov<sup>3</sup>

<sup>1,2,3</sup> Department of Electronic Technology in Engineering, Bauman Moscow State Technical University, Moscow, Russia  
Email: <sup>1</sup> mikhailov@bmstu.ru, <sup>2</sup> wertyoz@bk.ru, <sup>3</sup> kazalexander@mail.ru

\*Corresponding Author

**Abstract**—The most important task of ensuring the quality of operation of technological and research equipment is its effective protection from external vibration effects in the area of low frequencies, at which resonance phenomena are manifested. For this purpose, various types of vibration isolation systems are used, which are divided into passive and active. Passive systems effectively suppress vibrations at frequencies above 40-50 Hz, at lower frequencies such systems are ineffective as they cannot compensate for resonance phenomena. In this case, active vibration isolation systems are used. The active dampers and platform based on magnetorheological (MR) elastomers presented in the paper demonstrated higher vibration isolation efficiency in the frequency range of 0.3-3 Hz compared to the piezoelectric system and in the frequency range of 0.3-20 Hz compared to the platform based on electromagnetic power drive. At these frequencies, the vibration displacement amplitude transfer coefficient was less than 0.075. The use of MR effect makes it possible to regulate the stiffness and deformation of the elastic active element made of MR elastomer by changing the magnitude of magnetic induction. In this case it is possible to control dynamic and precision characteristics of the active damper, as well as to increase the efficiency of vibration isolation. During dynamic modelling of the active MP damper the differential equations and transfer functions of its elements were determined. Modelling in Simulink MATLAB software environment allowed to determine the transient process of damper movement under the influence of harmonic oscillations, select the type of regulator and calculate its tuning parameters. Experimental studies were carried out on a vibration test bench and confirmed the modelling results at frequencies of 0.3-50 Hz. At frequencies higher than 50 Hz passive vibration isolation begins to prevail due to absorption of vibration energy in the MR elastomer, which is not taken into account in the modelling. The experimental amplitude-frequency response of the platform showed high vibration isolation efficiency at frequencies of 0.3-100 Hz with vibration displacement amplitude transfer coefficient less than 0.075.

**Keywords**—Dynamic Modelling; Automatic Control; Active Vibration Isolation; Magnetorheological Elastomers; Amplitude-Frequency Characteristic.

## I. INTRODUCTION

Modern technologies of production and research of micro- and nanostructures (films, bulk structures), have a wide range of methods of formation and control of local surface properties, for which it is necessary to carry out work with a resolution of less than 100 nm [1]-[5]. Such technological and research equipment includes installations that use ion, electron or X-ray beams for surface processing and analysis (electron microscopes, scanning probe microscopes, equipment for micro- and nanolithography,

equipment for nanolocal ion and electron processing, etc.), as well as optical radiation (high-resolution optical microscopes, etc.). At the same time, the most important task of ensuring the quality of such equipment is its effective protection from external vibration effects in the low frequency range, at which resonance phenomena are manifested. It is especially important at intensive development of nanotechnologies, which are realised mainly due to the use of ultrahigh vacuum equipment, elements of which have low rigidity (thin-walled vacuum chambers, motion inputs into vacuum based on bellows, membranes, etc.) and, accordingly, low resonance frequencies.

For this purpose, different types of vibration isolation systems are used, which are divided into passive and active [6]-[10]. Passive systems effectively suppress vibrations at frequencies higher than 40-50 Hz, while in the low-frequency region such systems are ineffective because they cannot compensate for resonance phenomena. For vibration isolation in the low-frequency range, active vibration isolation systems that utilise the energy of an additional source are used. Modern systems combining active and passive vibration isolation are the most effective. Depending on the type of actuating mechanism, modern active systems can be divided into the following groups: hydraulic, pneumatic, electromagnetic, piezoelectric, magnetostrictive, elastomeric and others [11]-[48]. However, for them there is a problem of increasing the efficiency of vibration isolation at extremely low frequencies of vibration effects. Thus, the purpose of the conducted research was to increase the efficiency of vibration isolation at frequencies less than 20 Hz by using new materials - MR elastomers.

The MR active dampers and a platform based on them, controlled by a closed-loop microcontroller-based system presented in the paper, demonstrated high vibration isolation performance at frequencies of 0.3-100 Hz. The use of the MR effect makes it possible to adjust the stiffness coefficient of an elastic active element made of MR elastomer by changing the magnetic induction value. In this case it is possible to control the dynamic and precision characteristics of the active damper, as well as to increase the efficiency of vibration isolation of precision equipment [49]-[51]. The active damper has two functions: damper and actuator for moving and stabilising the position of the equipment to be protected. Thus, it operates in both passive and active vibration isolation modes. Passive mode is effective at vibration frequencies of more than 40-50 Hz, while active mode is effective at lower frequencies.



## II. DESCRIPTION OF THE ACTIVE VIBRATION ISOLATION PLATFORM

The scientific group of Bauman Moscow State Technical University has developed an active vibration isolation platform based on magnetorheological (MR) elastomers. [49]. Fig. 1 shows a photograph of the platform with top plate position sensors, while Fig. 2 shows a photograph of the platform without top plate, which contains four active one- or three-axis MR dampers 1 and four elastic suspension assemblies 2 with quasi-zero stiffness. The platform based on single-axis MR dampers provides three degrees of mobility: one linear vertical and two angular around horizontal axes. The platform based on three-axis MR dampers provides six degrees of mobility: three linear and three angular.

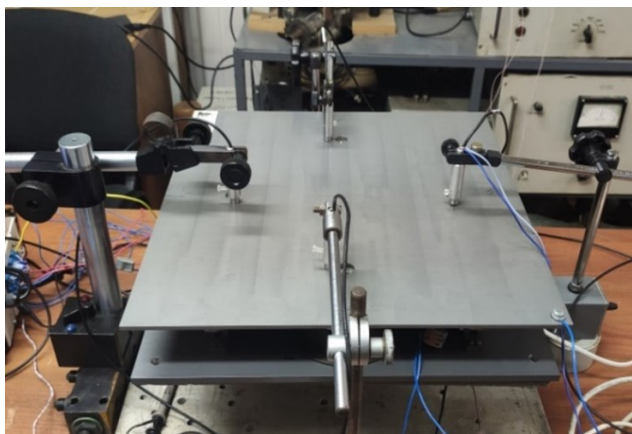


Fig. 1. Photograph of the platform with top plate movement sensors



Fig. 2. Photograph of the platform without the top plate: 1 - four active one- or three-axis MR dampers; 2 - four elastic suspension nodes with quasi-zero stiffness

MR elastomers are smart materials, which are composites based on silicone and micron-sized magnetic particles (e.g., carbonyl iron) [43]-[46]. Such materials can reversibly deform and change visco-plastic-elastic properties, such as elastic modulus, shear modulus and dynamic viscosity, when subjected to a magnetic field. These properties allow for improved damping compared to conventional viscoelastic systems. In addition, the active damper can be used as a micro- and nanopositioning actuator to move and stabilise the position of the vibration-isolated object.

The advantages of active vibration isolation systems using MR elastomers are a larger range of motion (up to 1 mm) compared to piezoelectric transducers and more effective absorption of vibration energy, the possibility of active control of amplitude-frequency characteristics and positioning with millisecond speed and nanometre accuracy of motion.

The platform consists of two plates, between which four active three-axis or single-axis MR dampers 1 and four elastic suspension assemblies 2 with quasi-zero stiffness are placed. In the design of the single-coordinate MR damper, the elastomeric element is in the form of a membrane, while in the three-axis MR damper it is in the form of a cup.

The single-axis MR damper contains an axial electromagnetic coil that produces a magnetic field in the axial direction. Under the action of the magnetic field, the movable rigid centre of the membrane moves in the axial direction. The movable rigid centres of the membranes of all four MR dampers are fixed to the top plate of the platform and move it axially.

The three-axis MR damper in the lower part contains an axial electromagnetic coil creating a magnetic field in the axial direction, the upper part has four horizontal electromagnetic coils creating a magnetic field in the radial direction, which allows the damper to be moved in both axial and horizontal directions.

## III. MODELLING OF AUTOMATIC CONTROL SYSTEM OF ACTIVE DAMPER

The equation of motion of the moving rigid centre of the MP damper membrane contains in the left part the inertial, viscous and elastic forces of resistance to motion, and in the right part the driving force from the magnetic field:

$$m_{red} \frac{d^2 Y(t)}{dt^2} + H \frac{dY(t)}{dt} + k = F_{mag}(t) \quad (1)$$

where  $Y(t)$  is displacement of the movable rigid centre along the longitudinal axis  $Y$ ;  $F_{mag}(t)$  is the axial force acting on the moving rigid centre of the MR elastomer membrane from the magnetic field side;  $m_{red}$  is reduced mass of the moving rigid centre of the membrane;  $H$  is viscous friction coefficient in MR elastomer;  $k$  is stiffness coefficient of MR elastomeric membrane or MR elastomeric cup.

The axial stiffness of the MR elastomeric cup consisting of a membrane and a tubular element under axial deformation under the action of a magnetic field was determined. This allowed to find the transfer function of the moving rigid centre of the active MR damper. The stiffness coefficient  $k_1$  of the MR elastomer membrane was determined experimentally. The stiffness coefficient  $k_2$  of the tubular element according to Maxwell's formula depends on the magnetic and mechanical characteristics of MR elastomer:

$$k_2 = \frac{S}{L} (9,81 \cdot 10^{12} \cdot (B/5000)^2 \varphi_v + E_{mre}^0) \quad (2)$$

where  $S$  is the cross-sectional area of the tubular element made of MR elastomer ( $m^2$ );  $L$  is the height of the tubular element made of MR elastomer (m);  $\varphi_v$  is the volume concentration of dispersed phase particles;  $B$  is the magnetic induction in MR elastomer (Tl);  $E_{MP}^0$  is the elastic modulus of MR elastomer in the absence of magnetic field (Pa). The magnetic induction  $B$  in MR elastomer depends on many factors: the size and distribution of dispersed phase particles in the elastomeric matrix, their relative magnetic

permeability, which is nonlinearly dependent on the magnetic field, the volume concentration of particles, etc. Thus, determination of the stiffness coefficient  $k_2$  by Maxwell's formula leads to a large error, so it is reasonable to find it as follows  $k_2 = \frac{E_{mre}S}{L}$ , where  $E_{mre}$  is the elastic modulus of MR elastomer under the action of magnetic field determined experimentally. The total stiffness coefficient  $k$  MR of the elastomeric cup is defined as the stiffness coefficient of the membrane and tubular element connected sequentially under axial load. The use of the MR effect makes it possible to adjust the total stiffness coefficient  $k$  of the elastic MR elastomeric cup by varying the magnitude of the magnetic induction  $B$ . In this case, the dynamic and accuracy characteristics of the active MR damper can be controlled. The stability of the tubular element made of MR elastomer can be improved.

Considering the Laplace transform of equation 1, the following equation is written:

$$Y(s) \cdot (m_{red}S^2 + HS + k) = F_{mag}(s) \quad (3)$$

where  $S$  is the Laplace function.

The transfer function of the moving rigid centre of the membrane is obtained:

$$W_C(s) = \frac{Y(s)}{F_{mag}(s)} = \frac{1}{m_{red}S^2 + HS + k} = \frac{\frac{1}{k}}{\frac{m_{red}}{k}S^2 + \frac{H}{k}S + 1} \quad (4)$$

$$= \frac{\frac{1}{k}}{T_{cor}^2S^2 + T_tS + 1}$$

where  $T_{cor}$  is the time constant of the moving core under the action of inertial and elastic forces ( $T_{cor} = \left(\frac{m_{red}}{k}\right)^{1/2}$ );  $T_t$  is the time constant of the moving rigid centre under the action of viscoelastic forces ( $T_t = H/k$ ).

Modelling of the developed automatic control system (ACS) of active MR damper with moving core position feedback in Simulink MATLAB software environment [52]-[64] has been carried out. In the course of modelling, the response of the system was analysed under simultaneous action of harmonic vibration disturbances and a stepped control signal with stepwise movement of the MR damper by 5  $\mu$ m. A comparison of the performance behaviour of three-axis and single-axis MR dampers under axial displacement was carried out, which showed similar dynamic performance with a slight reduction in the axial stiffness of the three-axis damper. At the same time, the transmission coefficient of vibration displacement amplitude for both models does not exceed 0.1 in the frequency range of 0.3-100 Hz. Modelling also allowed to choose control algorithms, structure and composition of the control system.

The structural scheme of ACS of one control channel of a three-axis MR-damper with proportional-integral-differentiating (PID) controller and feedback on the position of the moving core is shown in Fig. 3.

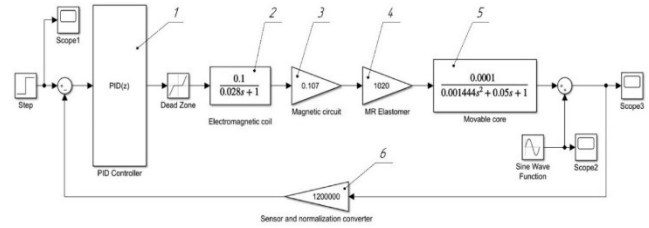


Fig. 3. Structural diagram of the system of automatic regulation of one control channel of the three-axis MR damper with PID-controller

PID-controller 1 is built after the signal combiner in sequence with ACS links of the MR damper: nonlinearity of the MR damper (dead zone), electromagnetic coil 2, magnetic core 3, MR elastomer 4, moving core 5, measuring system 6 of the moving core position. The transient process of ACS of three-axis MR damper under sinusoidal vibration action with vibration amplitude of 5  $\mu$ m and frequency of 5 Hz, with input step signal of 5  $\mu$ m is shown in Fig. 4. In this case, the frequency of vibration effects of 5 Hz is in the range of resonance frequencies of the platform for the active vibration isolation mode of the MMR-1 metallographic microscope (see Fig. 8).

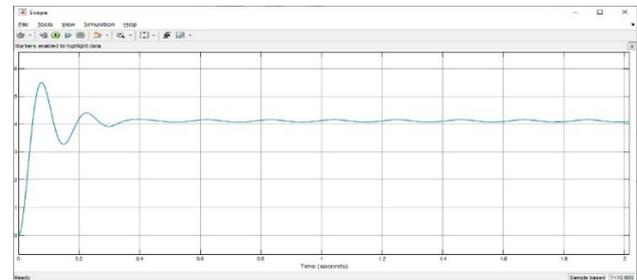


Fig. 4. Transient process of the automatic control system of the three-axis MR-damper

The transient time was no more than 0.3 s, with residual vibrations not compensated by the PID controller. The value of vibration displacement amplitude transfer coefficient (VDAC) is 0.05. The VDAC indicates what proportion of vibration displacement is transferred during vibration from the damper base to the moving rigid centre of the MP damper membrane. This parameter is important for evaluating the performance of the active platform as a whole, i.e. for assessing its vibration isolation properties:  $VDAC = \frac{A_1}{A_0}$ , where  $A_1$  is the amplitude of vibration displacements of the moving rigid centre of the MR damper membrane,  $A_0$  is the amplitude of vibration displacements of the damper base.

The modelling of the ACS performance of active MR dampers in the frequency range of 0.3-100 Hz was carried out and the results are shown in Table I.

Comparison of the results of ACS modelling of one-axis and three-axis MR dampers at axial displacement showed similar dynamic characteristics with a small decrease in axial stiffness of MR elastomeric cup in comparison with MR elastomeric diaphragm. Moreover, the difference in vibration amplitude reduction, defined as 20lg (VDAC) for these models, is no more than 3.6 dB for the entire frequency range of 0.3-100 Hz.

TABLE I. RESULTS OF MODELLING OF ACS OF ACTIVE MR-DAMPERS

Frequency, Hz	Single-axis MR damper		Three-axis MR damper	
	VDAC	20lg (VDAC), dB	VDAC	20lg (VDAC), dB
0.3	0.030	-30.4	0.025	-32
0.5	0.040	-27.9	0.040	-27.9
1	0.050	-26	0.040	-27.9
5	0.050	-26	0.050	-26
10	0.050	-26	0.040	-27.9
20	0.035	-29.1	0.030	-30.4
30	0.020	-33.9	0.020	-33.9
50	0.015	-36.4	0.010	-40
60	0.002	-53.9	0.002	-53.9
100	0.001	-60	0.001	-60

#### IV. TEST BENCH AND EXPERIMENTAL RESULTS

To investigate the active mode of vibration isolation with a closed-loop control system, a high-resolution metallographic microscope MMR-1 was selected as the protected object. A photograph of the bench for platform performance evaluation is shown in Fig. 5. Vibration effects on the platform base were set using a vibration test rig (not shown in Fig. 5). Readings from capacitive sensors located above the microscope slide and on the base of the platform were used to evaluate the performance of the platform. The data from the sensors were written to a file and processed according to a given algorithm to determine the VDAC for a closed-loop automatic control system based on a microcontroller.

Experimental studies of the active damper and platform were carried out to determine the operating modes of the system, to carry out ACS tuning and to demonstrate the effectiveness of the active vibration isolation platform with closed-loop control system. Closed-loop ACS moves single-coordinate MR dampers in counter-phase to external disturbances. The use of position feedback in the ACS scheme significantly increases the accuracy of the system, but reduces its speed. To determine the fast performance, the balance of the components of the transient time was analysed when working off the movement of the active damper in counter-phase to external influences under the control of the STM32 microcontroller. As a result of the analysis it was found that the transients last less than 10 ms, which is sufficient for effective vibration isolation in the full frequency range from 0.3 to 100 Hz.

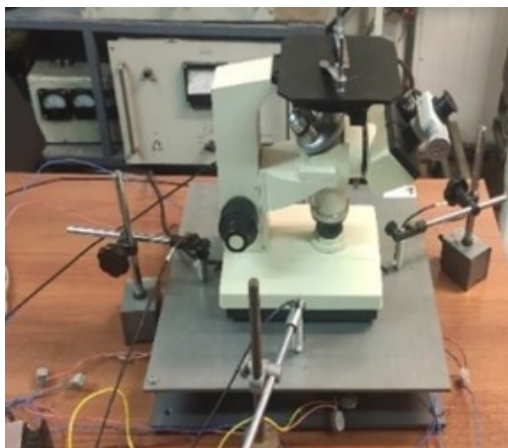


Fig. 5. General view of the bench for vibration isolation research using metallographic microscope MMR-1

The amplitude-frequency response of the microscope was analysed beforehand, i.e. the amplitude of vibrations transmitted to the microscope slide from the base under external vibrations with an amplitude of 0.3 mm in the frequency range of 0.3-100 Hz. The diagram of the amplitude-frequency response is shown in Fig. 6. The graph shows that the resonant frequencies of the MMR-1 metallographic microscope are in the range of 10-18 Hz, and the peak value of the resonant frequency is 13 Hz.

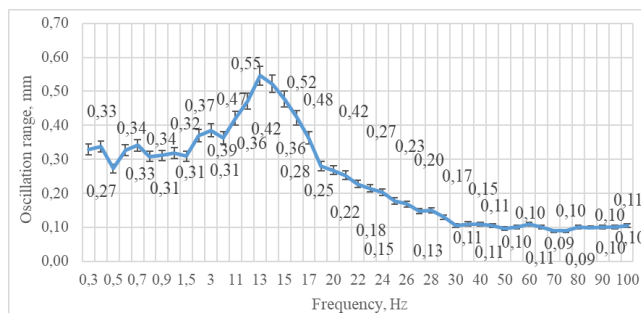


Fig. 6. Amplitude-frequency characteristic of the MMR-1 metallographic microscope

In the research of active mode vibration isolation of the MMR-1 microscope, experiments were conducted in the frequency range from 0.3 to 100 Hz. The vibration displacement amplitude transfer coefficient (VDAC) as a function of the frequency of external disturbances for a closed-loop automatic control system based on an STM32 microcontroller is calculated for the entire frequency range. Fig. 7 demonstrates the effectiveness of the active vibration isolation system at the resonant frequency of the MMR-1 metallographic microscope of 13 Hz, for which it was possible to reduce the external vibrations transmitted to the slide of the MMR-1 metallographic microscope from an amplitude of 318  $\mu\text{m}$  to 20-26  $\mu\text{m}$ .

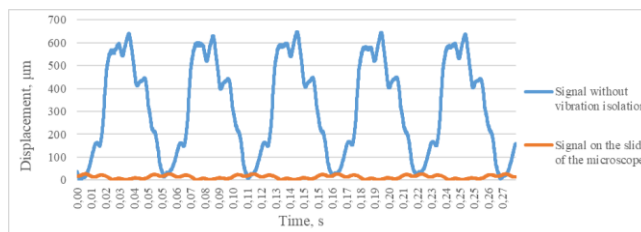


Fig. 7. Diagram of time dependence of displacement of the MMR-1 microscope stage at active vibration isolation and without vibration isolation for the resonance frequency of 13 Hz

Experiments were conducted in the frequency range from 0.3 to 100 Hz, with a maximum vibration disturbance spread of 600  $\mu\text{m}$ . Fig. 8 shows a graph of the dependence of the vibration displacement amplitude transfer coefficient (VDAC) of the platform on the external disturbance frequency for the active vibration isolation mode of the MMR-1 metallographic microscope.

The graph shows high efficiency of the active vibration isolation system. In this case, the maximum value of the transmission coefficient of the displacement amplitude in the whole investigated frequency range does not exceed 0.071.



- Control Systems Technology*, vol. 29, no. 4, pp. 1674–1688, Jul. 2021, doi: 10.1109/tcst.2020.3022951.
- [11] J. Li, X. Lv, L. Liu, Y. Liu, and J. Leng, “Computational model and design of the soft tunable lens actuated by dielectric elastomer,” *Journal of Applied Mechanics*, vol. 87, no. 7, May 2020, doi: 10.1115/1.4046896.
- [12] M. Grasinger and K. Dayal, “Statistical mechanical analysis of the electromechanical coupling in an electrically-responsive polymer chain,” *Soft Matter*, vol. 16, no. 27, pp. 6265–6284, 2020, doi: 10.1039/d0sm00845a.
- [13] H. Medina and C. W. Farmer, “Improved model for conical dielectric elastomer actuators with fewer electrical connections,” *Journal of Mechanisms and Robotics*, vol. 12, no. 3, Feb. 2020, doi: 10.1115/1.4045651.
- [14] H. Li, L. Chen, C. Zhao, and S. Yang, “Evoking or suppressing electromechanical instabilities in soft dielectrics with deformation-dependent dielectric permittivity,” *International Journal of Mechanical Sciences*, vol. 202–203, p. 106507, Jul. 2021, doi: 10.1016/j.ijmecsci.2021.106507.
- [15] N. Ma, X. Dong, J. C. Arreguin, C. Bishop, and D. Axinte, “A class of novel underactuated positioning systems for actuating/configuring the parallel manipulators,” *Robotica*, vol. 40, no. 10, pp. 3631–3650, Apr. 2022, doi: 10.1017/s0263574722000431.
- [16] L. Wu, A. Müller, and J. S. Dai, “A matrix method to determine infinitesimally mobile linkages with only first-order infinitesimal mobility,” *Mechanism and Machine Theory*, vol. 148, p. 103776, Jun. 2020, doi: 10.1016/j.mechmachtheory.2019.103776.
- [17] C. Huang, Z. Lai, L. Zhang, X. Wu, and T. Xu, “A magnetically controlled soft miniature robotic fish with a flexible skeleton inspired by zebrafish,” *Bioinspiration & Biomimetics*, vol. 16, no. 6, p. 065004, Sep. 2021, doi: 10.1088/1748-3190/ac23a9.
- [18] Y. Kim and X. Zhao, “Magnetic soft materials and robots,” *Chemical Reviews*, vol. 122, no. 5, pp. 5317–5364, Feb. 2022, doi: 10.1021/acs.chemrev.1c00481.
- [19] T. Ashuri, A. Armani, R. Jalilzadeh Hamidi, T. Reasnor, S. Ahmadi, and K. Iqbal, “Biomedical soft robots: current status and perspective,” *Biomedical Engineering Letters*, vol. 10, no. 3, pp. 369–385, May 2020, doi: 10.1007/s13534-020-00157-6.
- [20] C. Li *et al.*, “Fast and programmable locomotion of hydrogel-metal hybrids under light and magnetic fields,” *Science Robotics*, vol. 5, no. 49, Dec. 2020, doi: 10.1126/scirobotics.abb9822.
- [21] C. Lee *et al.*, “Soft robot review,” *International Journal of Control, Automation and Systems*, vol. 15, no. 1, pp. 3–15, Jan. 2017, doi: 10.1007/s12555-016-0462-3.
- [22] H.-S. Lee *et al.*, “Wireless walking paper robot driven by magnetic polymer actuator,” *Actuators*, vol. 9, no. 4, p. 109, Oct. 2020, doi: 10.3390/act9040109.
- [23] C. S. X. Ng, M. W. M. Tan, C. Xu, Z. Yang, P. S. Lee, and G. Z. Lum, “Locomotion of miniature soft robots,” *Advanced Materials*, vol. 33, no. 19, Dec. 2020, doi: 10.1002/adma.202003558.
- [24] G. Stano and G. Percoco, “Additive manufacturing aimed to soft robots fabrication: A review,” *Extreme Mechanics Letters*, vol. 42, p. 101079, Jan. 2021, doi: 10.1016/j.eml.2020.101079.
- [25] H. Chung, A. M. Parsons, and L. Zheng, “Magnetically controlled soft robotics utilizing elastomers and gels in actuation: A review,” *Advanced Intelligent Systems*, vol. 3, no. 3, Dec. 2020, doi: 10.1002/aisy.202000186.
- [26] N. Bira, P. Dhagat, and J. R. Davidson, “A review of magnetic elastomers and their role in soft robotics,” *Frontiers in Robotics and AI*, vol. 7, Oct. 2020, doi: 10.3389/frobt.2020.588391.
- [27] N. El-Atab *et al.*, “Soft actuators for soft robotic applications: A review,” *Advanced Intelligent Systems*, vol. 2, no. 10, Aug. 2020, doi: 10.1002/aisy.202000128.
- [28] S. Kolachalama and S. Lakshmanan, “Continuum robots for manipulation applications: A survey,” *Journal of Robotics*, vol. 2020, pp. 1–19, Jul. 2020, doi: 10.1155/2020/4187048.
- [29] K. Maeda, H. Shinoda, and F. Tsumori, “Miniaturization of worm-type soft robot actuated by magnetic field,” *Japanese Journal of Applied Physics*, vol. 59, Mar. 2020, doi: 10.35848/1347-4065/ab7b18.
- [30] I. Bica and E. M. Anitas, “Graphene platelets-based magnetoactive materials with tunable magnetoelectric and magnetodielectric properties,” *Nanomaterials*, vol. 10, no. 9, p. 1783, Sep. 2020, doi: 10.3390/nano10091783.
- [31] M. Bunoiu, E. M. Anitas, G. Pascu, L. M. E. Chirigiu, and I. Bica, “Electrical and magnetodielectric properties of magneto-active fabrics for electromagnetic shielding and health monitoring,” *International Journal of Molecular Sciences*, vol. 21, no. 13, p. 4785, Jul. 2020, doi: 10.3390/ijms21134785.
- [32] T. I. Becker, O. V. Stolbov, D. Y. Borin, K. Zimmermann, and Y. L. Raikher, “Basic magnetic properties of magnetoactive elastomers of mixed content,” *Smart Materials and Structures*, vol. 29, no. 7, p. 075034, Jun. 2020, doi: 10.1088/1361-665x/ab8fc9.
- [33] D. V. Saveliev *et al.*, “Giant extensional strain of magnetoactive elastomeric cylinders in uniform magnetic fields,” *Materials*, vol. 13, no. 15, p. 3297, Jul. 2020, doi: 10.3390/ma13153297.
- [34] D. Takahashi *et al.*, “Magnetorheological response for magnetic elastomers containing carbonyl iron particles coated with Poly(methyl methacrylate),” *Polymers*, vol. 13, no. 3, p. 335, Jan. 2021, doi: 10.3390/polym13030335.
- [35] A. K. Bastola and M. Hossain, “A review on magneto-mechanical characterizations of magnetorheological elastomers,” *Composites Part B: Engineering*, vol. 200, p. 108348, Nov. 2020, doi: 10.1016/j.compositesb.2020.108348.
- [36] E. Y. Kramarenko, G. V. Stepanov, and A. R. Khokhlov, “Magnetically active silicone elastomers: Twenty years of development,” *INEOS Open*, vol. 2, pp. 178–184, 2020.
- [37] H. H. Valiev, V. M. Cherepanov, Y. N. Karnet, A. J. Minaev, and G. V. Stepanov, “Atomic force microscopy and Mössbauer spectroscopy of magnetically active silicone elastomers,” *IOP Conference Series: Materials Science and Engineering*, vol. 862, no. 2, p. 022062, May 2020, doi: 10.1088/1757-899x/862/2/022062.
- [38] A. J. Minaev, J. V. Korovkin, G. V. Stepanov, and H. H. Valiev, “Studies on dynamic deformations of magnetorheological elastomer,” *Journal of Physics: Conference Series*, vol. 1546, no. 1, p. 012136, May 2020, doi: 10.1088/1742-6596/1546/1/012136.
- [39] M. Watanabe, Y. Tanaka, D. Murakami, M. Tanaka, M. Kawai, and T. Mitsumata, “Optimal plasticizer content for magnetic elastomers used for cell culture substrate,” *Chemistry Letters*, vol. 49, no. 3, pp. 280–283, Mar. 2020, doi: 10.1246/cl.190929.
- [40] A. M. Sergeev, A. A. Solovyev, and N. S. Kovalev, “Smart prosthesis: Sensorization, humane vibration and processor control,” *Advances in Intelligent Systems and Computing*, pp. 477–486, Aug. 2020, doi: 10.1007/978-3-030-55506-1\_43.
- [41] J. Kim, D. W. Seo, K. S. Jung, and K. T. Park, “Development of inspection robot for removing snow on stays of cable-stayed bridge,” *Journal of the Korea Academia-Industrial Cooperation Society*, vol. 21, no. 3, pp. 246–252, 2020.
- [42] Z. Hong, K. He, Y. Xu, H. Fang, Q. Zuo, and Z. Li, “Design and research on impact deicing mechanism of cable climbing robot,” in *Proc. 2021 International Conference on Computer, Control and Robotics (ICCCR)*, Jan. 2021, doi: 10.1109/icccr49711.2021.9349271.
- [43] A. Ja Minaev and J. V. Korovkin, “Creation of a magnetoelastic material deformation,” *Journal of Physics: Conference Series*, vol. 1889, no. 2, p. 022111, Apr. 2021, doi: 10.1088/1742-6596/1889/2/022111.
- [44] M. Cvek, A. Zahoranova, M. Mrlik, P. Sramkova, A. Minarik, and M. Sedlacik, “Poly(2-oxazoline)-based magnetic hydrogels: Synthesis, performance and cytotoxicity,” *Colloids and Surfaces B: Biointerfaces*, vol. 190, p. 110912, Jun. 2020, doi: 10.1016/j.colsurfb.2020.110912.
- [45] D. Borin, G. Stepanov, A. Musikhin, A. Zubarev, A. Bakhtiarov, and P. Storozhenko, “Magnetorheological effect of magnetoactive elastomer with a permalloy filler,” *Polymers*, vol. 12, no. 10, p. 2371, Oct. 2020, doi: 10.3390/polym12102371.
- [46] D. Y. Borin and M. V. Vaganov, “FORC analysis of magnetically soft microparticles embedded in a polymeric elastic environment,” *Journal of Physics D: Applied Physics*, vol. 55, no. 15, p. 155001, Jan. 2022, doi: 10.1088/1361-6463/ac48b1.
- [47] D. Yu. Borin, C. Bergmann, and S. Odenbach, “Characterization of a magnetic fluid exposed to a shear flow and external magnetic field

- using small angle laser scattering,” *Journal of Magnetism and Magnetic Materials*, vol. 497, p. 165959, Mar. 2020, doi: 10.1016/j.jmmm.2019.165959.
- [48] A. Zubarev, D. Chirikov, and D. Borin, “Internal structures and elastic properties of dense magnetic fluids,” *Journal of Magnetism and Magnetic Materials*, vol. 498, p. 166129, Mar. 2020, doi: 10.1016/j.jmmm.2019.166129.
- [49] V. P. Mikhailov, A. M. Bazinenkov, and A. V. Kazakov, “Active vibration isolation of nanotechnology equipment,” *IOP Conference Series: Materials Science and Engineering*, vol. 709, no. 4, p. 044046, Jan. 2020, doi: 10.1088/1757-899x/709/4/044046.
- [50] V. P. Mikhailov and A. M. Bazinenkov, “Study on adjustment and vibration isolation system for adaptive optics,” *Research Trends and Challenges in Physical Science*, vol. 8, pp. 73–82, Mar. 2022, doi: 10.9734/bpi/rtcps/v8/1940b.
- [51] A. M. Bazinenkov, D. A. Ivanova, A. P. Rotar’, and V. P. Mikhailov, “Actuator based on a dielectric elastomer with quartz as a filler for vacuum technology,” *IOP Conference Series: Materials Science and Engineering*, vol. 781, no. 1, p. 012007, Apr. 2020, doi: 10.1088/1757-899x/781/1/012007.
- [52] D. S. Ershov, A. V. Malakhov, A. V. Talalai, and R. Z. Khayrullin, “Analysis of operation models of complex technical systems,” *Measurement Techniques*, vol. 66, no. 7, pp. 461–474, Oct. 2023, doi: 10.1007/s11018-023-02248-z.
- [53] A. A. Gulnyashkin and A. G. Leskov, “Simulation of a six-rod mobile tensegrity robot in MATLAB environment,” *AIP Conference Proceedings*, vol. 2833, no. 1, 2023, doi: 10.1063/5.0151733.
- [54] T. Ono, R. Eto, J. Yamakawa, and H. Murakami, “Analysis and control of a Stewart platform as base motion compensators - Part I: Kinematics using moving frames,” *Nonlinear Dynamics*, vol. 107, no. 1, pp. 51–76, Nov. 2021, doi: 10.1007/s11071-021-06767-8.
- [55] A. K. Jishnu, D. K. S. Chauhan, and P. R. Vundavilli, “Design of neural network-based adaptive inverse dynamics controller for motion control of stewart platform,” *International Journal of Computational Methods*, vol. 19, no. 8, Mar. 2022, doi: 10.1142/s021987622142010x.
- [56] M. I. Hosseini, S. A. Khalilpour, and H. D. Taghirad, “Practical robust nonlinear PD controller for cable-driven parallel manipulators,” *Nonlinear Dynamics*, vol. 106, no. 1, pp. 405–424, Aug. 2021, doi: 10.1007/s11071-021-06758-9.
- [57] V. A. Glazunov, P. A. Laryushkin, and K. A. Shalyukhin, “Structure, kinematics, and prototyping of a parallel manipulator with a remote center of rotation,” *Journal of Machinery Manufacture and Reliability*, vol. 52, no. 6, pp. 585–591, Dec. 2023, doi: 10.1134/s1052618823060080.
- [58] R. Liu, F. Nageotte, P. Zanne, M. de Mathelin, and B. Dresp-Langley, “Deep reinforcement learning for the control of robotic manipulation: A focussed mini-review,” *Robotics*, vol. 10, no. 1, p. 22, Jan. 2021, doi: 10.3390/robotics10010022.
- [59] I. K. Romanova-Bolshakova and E. V. Poleschikov, “Reconfigurable wheeled walking robot with adaptive control,” *AIP Conference Proceedings*, vol. 2833, no. 1, 2023, doi: 10.1063/5.0151970.
- [60] D. Rawat, M. K. Gupta, and A. Sharma, “Intelligent control of robotic manipulators: a comprehensive review,” *Spatial Information Research*, vol. 31, no. 3, pp. 345–357, Dec. 2022, doi: 10.1007/s41324-022-00500-2.
- [61] V. S. D. M. Sahu, P. Samal, and C. Kumar Panigrahi, “Modelling, and control techniques of robotic manipulators: A review,” *Materials Today: Proceedings*, vol. 56, pp. 2758–2766, 2022, doi: 10.1016/j.matpr.2021.10.009.
- [62] A. P. Singh, D. Deb, H. Agrawal, K. Bingi, and S. Ozana, “Modeling and Control of Robotic Manipulators: A fractional calculus point of view,” *Arabian Journal for Science and Engineering*, vol. 46, no. 10, pp. 9541–9552, Feb. 2021, doi: 10.1007/s13369-020-05138-6.
- [63] Z. Liu, K. Peng, L. Han, and S. Guan, “Modeling and control of robotic manipulators based on artificial neural networks: A review,” *Iranian Journal of Science and Technology, Transactions of Mechanical Engineering*, vol. 47, no. 4, pp. 1307–1347, Jan. 2023, doi: 10.1007/s40997-023-00596-3.
- [64] T.-T. Do, V.-H. Vu, and Z. Liu, “Linearization of dynamic equations for vibration and modal analysis of flexible joint manipulators,” *Mechanism and Machine Theory*, vol. 167, p. 104516, Jan. 2022, doi: 10.1016/j.mechmachtheory.2021.104516.